구조 소음저감을 위한 격자 패널의 다중 진동제어

김인수*, 김영식*

Multiple Vibration Control of a Trim Panel to Reduce Structure-borne Noise

In-Soo Kim* and Yeung-Shik Kim*

ABSTRACT

본 연구에서는 격자패널을 통한 소음전달을 감소시키기 위하여 외부 구조적 가진으로부터 유발된 경량 패널의 진동을 능동 제어하는 기법을 기술한다. 최적 되먹임제어기와 적응 앞먹임제어기가 결합된 혼합형 제어기가 진동제어기로 사용된다. 되먹임제어기는 주파수영역의 모델규명법에 의해 추출된 다중 입/출력 패널진동계 모델에 대하여 LQG 최적기법을 이용하여 감쇠능을 향상시키도록 설계된다. 앞먹임제어기는 되먹임 궤환의 결합효과를 자동적으로 보정할 수 있는 제안된 학습법칙에 기초하여 패널의 잔류진동이 최소가 되도록 적용된다. 45.7 × 45.7×2.54 cm^3 벌집형상의 고강도 패널, 4개의 관성형 구동기 및 이산신호처리장치에 의해 구현된 패널 진동계에 대한 능동제어 실험을 수행해 본 결과 600Hz 주파수대역에 대한 12dB 진동저감이 이루어 질 수 있었다.

Key Words : Active Trim Panel(능동 격자 패널), Hybrid Controller(혼합형 제어기), Sound Transmission Loss(음향 투과손실), Multiple Vibration Control(다중 진동제어)

1. Introduction

The active control of interior noise fields in aircraft cabin induced by structural excitation has been an ongoing technical challenge. Several active control techniques have been focused on the reduction of low frequency noise since the use of passive means is only effective for high frequency noise field[1]. Generally, active control of interior noise fields uses destructive interference of sound waves and thus requires many sources and sensors distributed in the internal space. Fuller[2] described that for low modal densities, only a few actuators attached to a vibrating panel can change its sound radiation characteristics and achieve large reductions in radiated sound levels. Noise reduction can be obtained not only by the suppression of the vibration amplitude of a panel but by changing its response so as to vibrate with a lower radiation efficiency (modal restructuring). Thomas[3] predicted analytically that the considerable noise attenuation could be achieved using only three actuators when controlling a single rigid plate (having only rigid body modes). If the motion is restricted to its out-of -plane piston mode. only one actuator is needed and the need for modal restructuring is eliminated because only the amplitude of motion needs to be reduced. Using a control panel vibrating in a piston-like mode. St. Pierre[4] was able to reduce sound transmission through a composite panel using its volume

* 금오공과대학교 기계공학부

velocity as the quantity to be minimized in the control error function.

Active vibration control schems can be divided into two categories: feedback and feedforward control. Feedback control can be used when a reference signal coherent with primary disturbance is not available. The various feedback-based controllers such as modal space control, linear quadratic Gaussian (LQG) and H∞ optimal posses a good performance in damping increase and transient suppression[5-7]. However, most feedback controllers with fixed coefficients often lead to stability and robustness problems due to small variations of plant dynamics. Recent researches in adaptive feedforward controller including filtered-x and filtered-u least-mean-square (LMS) algorithms showed that robust performance in persistent disturbance rejection, such as the residual error typically driven to zero, can be achieved with little prior knowledge of plant dynamics[8,9]. Snyder and Kim showed that the convergence of these algorithm depends on the plant dynamics and its model error[10-13]. Nelson[14] introduced the multiple LMS algorithm available to the multiple input and multiple output (MIMO) plant. Saunders[15] described that hybrid structural control approach of single input and single output (SISO) plant can be applied for the rejection of harmonic or impulsive disturbance.

In this paper, we have purposely designed as trim panel to be as stiff and light as possible and constrained in such a way as to allow only rigid body modes. By embedding inertial actuators near its peripheries, the intention is to minimize the response of the trim panel's rigid body modes, and thus control its transmitted structure-borne sound. This approach allows for global noise reduction using local vibration control algorithms of the trim panel, provided that structural coupling between panels is held to minimum and all of the sound transmission paths into an enclosure are intercepted with such an active panel. A hybrid controller composed of an adaptive feedforward and an optimal feedback loop is used to reduce the vibration level of the panel. The feedback controller improves transient response characteristics on external disturbance by actively increasing the damping capacity of plant. Feedback

controller is designed using LQG technique based on MIMO model identified by a frequency domain curve fitting. The adaptation rule for hybrid controller which automatically compensates the effect of feedback link is proposed to maintain the control performance. The active vibration control system for the honeycomb composite panel, which is supported with soft rubber mounts, and driven by four inertia-type actuators, is presented using digital signal processing unit with 4 parallel high speed processors.

2. Design of Active Vibration Controller

2.1 Feedforward Control Using multiple Filtered-x LMS Algorithm

Figure 1 shows block diagram of a feedforward vibration control using multiple filtered-x LMS algorithm. Residual vibration $e_n(k)$ at n-th sensor is the result of destructive interference between the external disturbance and vibration created by control force.
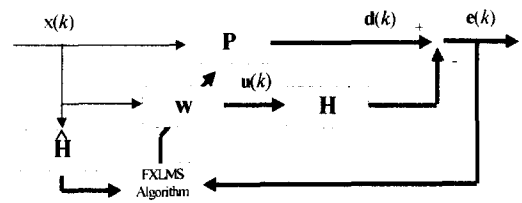

Fig. 1 Block diagram of single-reference/multiple output FXLMS algorithm

Secondary plant which includes dynamic characteristics between m-th acuator and n-th sensor including an anti-aliasing filter, and a transmission path of the structural vibration may be modeled by a finite impulse response (FIR) filter of order p. $H_{nm} = [h_{nm}(0), h_{nm}(1), ..., h_{nm}(p)]^T$. Assuming that m-th adaptive controller is represented by another FIR filter of order q. $W_{m,k} = [w_{m,k}(0), w_{m,k}(1),...,w_{m,k}(q)]^T$ where subscript k denotes the time at which the filter coefficients are updated, then $e_n(k)$ can be expressed as follows:

$$e_n(k) = d_n(k) - \sum_{m=1}^{M}\sum_{j=0}^{p}\sum_{i=0}^{q} h_{nm}(j)w_{m,k-j}(i)x(k-j-i).$$

$$(n=1,2,...,N) \tag{1}$$

where desired signal $d_n(k)$ is the vibration level induced by only external disturbance at the n-th sensor. $x(k)$ is the single reference input which is closely coherent with external disturbance but not corrupted by actuator force, e.g., blade rotational signal for a rotorcraft. $d_n(k)$ is represented using primary plant between external disturbance and n-th sensor which is modeled by FIR filter of order l, $P_n = [p_n(0), p_n(1), ..., p_n(l)]^T$,

$$d_n(k) = \sum_{i=1}^{l} P_n(i)x(k-i) . \qquad (2)$$

Coefficients of controller may be updated recursively based on the gradients of instantaneous squared residual vibration as follows:

$$w_{m,k+1}(i) = w_{m,k}(i) - \mu \frac{\partial \sum_{n=1}^{N} e_n^2(k)}{\partial w_{m,k}(i)}$$

$$= w_{m,k}(i) - 2\mu \sum_{n=1}^{N} e_n(k) \frac{\partial e_n(k)}{\partial w_{m,k}(i)} \quad (i=0,1,...,q), \quad (3)$$

where μ is a convergence factor that determines the speed of adaptation. Substitution of equation (1) into equation (3) yields the adaptation rule of the controller as follows:

$$w_{m,k+1}(i) = w_{m,k}(i) - 2\mu \sum_{n=1}^{N} e_n(k) \cdot$$

$$\frac{\partial \{ \sum_{m=1}^{M} \sum_{j=0}^{p} \sum_{i=0}^{q} h_{nm}(j)w_{m,k-j}(i)x(k-j-i) \}}{\partial w_{m,k}(i)} \qquad (4)$$

Since the partial derivative in the above equation cannot be given in an explicit form, it is assumed heuristically that the filter coefficients in past may be the same as the current ones

$$w_{m,k-j}(i) = w_{m,k}(i), \quad (j=0,1,...,p). \qquad (5)$$

This assumption may be reasonable one if the filter coefficients are updated slowly on a time-scale which is long compared with the dynamic response of secondary plant H_{nm}. Substitution of equation (5) into equation (4) yields the adaptation rule of the controller as follows:

$$w_{m,k+1}(i) = w_{m,k+1}(i) + 2\eta \sum_{n=1}^{N} e_n(k) \sum_{j=0}^{p} h_{nm}(j)x(k-j-i)$$

$$= w_{m,k}(i) + 2\eta \sum_{n=1}^{N} e_n(k)f_{nm}(k-i) \qquad (6)$$

where η is given by $\eta = (p+1)\mu$. f_{nm} is the filtered-x signal by filtering the reference input with secondary pant H_{nm},

$$f_{nm}(k-i) = \sum_{j=0}^{p} h_{nm}(j)x(k-j-i) . \qquad (7)$$

This is so called multiple filtered-X LMS algorithm which uses single reference input, multiple secondary plants and multiple residual vibrations in order to update multiple controllers. Snyder [10] surveyed the convergence characteristics of the iterative steepest descent algorithm which is derived under the assumption that reference input signal is stationary and random process, and may be impractical due to practical problems like unavailability of computing facility associated with matrix manipulation. The stability criteria of the filtered-x LMS algorithm is derived under the assumption of slow adaptation of filter coefficients represented with equation (5). Define a semi-positive definite quadratic Lyapunov function[16] $V(k)$ as follows:

$$V(k) = \frac{1}{4\eta} \sum_{m=1}^{M} \sum_{i=0}^{q} (w_{m,k}(i) - w_m^*(i))^2 \geq 0 \qquad (8)$$

where $w_m^*(i)$ is the optimal filter of $w_{m,k}(i)$ [17] and $\eta > 0$. The function $V(k+1)$ can be derived using equations (6) to (8) as follows:

$$V(k+1) = V(k) + \eta \sum_{m=1}^{M} \sum_{i=0}^{q} \{ \sum_{n=1}^{N} e_n(k)f_{nm}(k-i) \}^2$$

$$+ \sum_{m=1}^{M} \sum_{i=0}^{q} \{ w_{m,k}(i) - w_m^*(i) \} \sum_{n=1}^{N} e_n(k)f_{nm}(k-i) \qquad (9)$$

Since residual vibration is given by following equation,

$$e_n(k) = \sum_{m=1}^{M}\sum_{i=0}^{q}\{w_m^*(i) - w_{m,k}(i)\}f_{nm}(k-i) \qquad (10)$$

equation (9) can be simplified to

$$V(k+1) = V(k) + \eta\sum_{m=1}^{M}\sum_{i=0}^{q}\{\sum_{n=1}^{N}e_n(k)f_{nm}(k-i)\}^2$$
$$- \sum_{n=1}^{N}e^2{}_n(k). \qquad (11)$$

Applying the Lyapunov stability criterion that $V(k+1)$ must be less than $V(k)$ yields the stability condition of η as follows:

$$0 < \eta < \frac{\displaystyle\sum_{n=1}^{N}e_n^2(k)}{\displaystyle\sum_{m=1}^{M}\sum_{i=0}^{q}\sum_{n=1}^{N}\{\sum e_n(k)f_{nm}(k-i)\}^2} \qquad (12)$$

In case of single input single output (SISO) plant, namely M=N=1. stable range of η is represented in the following brief form:

$$0 < \mu < \frac{1}{\displaystyle\sum_{i=0}^{q}f^2(k-i)} \qquad (13)$$

After the coefficients of adaptive controller is converged, the filtered-x signal may be assumed with variance σ_f^2 if external disturbance is under stationary process. Since $\sum_{i=0}^{q}f^2(k-i)$ of equation (13) is equal to $(q+1)\sigma_f^2$ or $\mathrm{Tr}(R_f)$ for the active control process under such a condition, equation (13) is identical with the stability criterion of iterative steepest descent algorithm. $\mathrm{Tr}(R_f)$ denotes the trace of auto-covariance matrix of filtered-x signal. Equations (12) and (13) mean that convergence factor of filtered-x LMS algorithm should be set inverse proportionally to the magnitude of filtered-x signal or impulse response of secondary plant H_{nm}. Therefore if external disturbance is consisted of the frequency components near to resonance of the secondary plant, feedforward controller adapted by

filtered-x LMS algorithm would converge very slowly and be unsuitable for the control of frequently changing external disturbance.

2.2 Hybrid Control

As pointed out in previous section, the filtered-x LMS algorithm may converge slowly in case that the secondary plant is a lightly damped system over the frequency band of external disturbance. In order to increase the convergence speed of the adaptive feedforward controller, a feedback controller may be used to improve the dynamics of secondary plant, such as increasing the damping capacity. This is the basic idea of proposed algorithm related with the design of hybrid controller.

2.2.1 Adaptive Feedforward Controller Combined With Feedback Loop

Figure 2 shows the block diagram of a hybrid adaptive control system. G denotes feedback controller which outputs control signal using only residual vibration $E(j\omega) = [E_1(j\omega), E_2(j\omega),...,E_N(j\omega)]^T$. The behavior of hybrid controller may be analyzed conveniently in frequency domain to get insight about hybrid control process. The control signal vector $U(j\omega)$ consists of the feedback signal $U_G(j\omega) = [U_{G1}(j\omega), U_{G2}(j\omega), ..., U_{GM}(j\omega)]^T$ and feedforward signal $U_W(j\omega) = [U_{W1}(j\omega), U_{W2}(j\omega), ..., U_{WM}(j\omega)]^T$ (the term $j\omega$ will be abbreviated for compact expression in following equations in this section).

$$U = U_G + U_W$$
$$= -GE + WX \qquad (14)$$
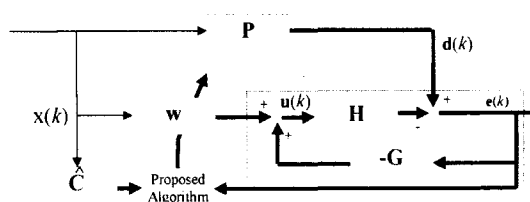
where G has N × M number of components.

Fig. 2 Block diagram of the single reference/multiple output hybrid feedback and adaptive feedforward control system

G_{nm} denotes the transfer function of feedback controller between n-th residual e_n and m-th feedback control signal U_{Cm}

$$G = \begin{bmatrix} G_{11} & G_{12} & \cdots & G_{1N} \\ G_{21} & G_{22} & \ldots & G_{2N} \\ \vdots & \vdots & \ddots & \vdots \\ G_{M1} & G_{M2} & \cdots & G_{MN} \end{bmatrix}, \quad (15)$$

and feedforward controller $W = [W_1, W_2, ..., W_M]^T$ generates feedforward control signal using single reference input. Residual vibration is the result of destructive interference between primary disturbances, $D = [D_1, D_2, ..., D_N]^T$ and secondary vibration signals at sensors.

$$E = D - HU \quad (16)$$

where H consists of H_{nm} which denotes secondary plant between m-th actuator and n-th sensor

$$H = \begin{bmatrix} H_{11} & H_{12} & \cdots & H_{1M} \\ H_{21} & H_{22} & \cdots & H_{2M} \\ \vdots & \vdots & \ddots & \vdots \\ H_{N1} & H_{N2} & \cdots & H_{NM} \end{bmatrix}. \quad (17)$$

Combining equation (14) with equation (16) yields the following equation.

$$E = (I_{N \times N} - HG)^{-1} D - (I_{N \times N} - HG)^{-1} HWX. \quad (18)$$

If feedforward controller is updated based on the complex gradient of $J = E^* E$ with regard to W, the following adaptation rule in frequency domain for feedforward controller is derived:

$$W(k+1) = W(k) + 2\gamma [(I_{N \times N} - HG)^{-1} HX]^* E(k) \quad (19)$$

where superscript * denotes the conjugate transpose. Equation (19) shows that when feedforward controller is combined with feedback loop, feedforward controller should be adapted based on the other filtered-x signal which is estimated using closed-loop transfer function $C = (I_{N \times N} - HG)^{-1} H$ instead of secondary plant H. Equation (19) can be converted into the new adaptation rule in time domain available for multiple feedforward

controllers with feedback loop.

$$w_{m,k+1}(i) = w_{m,k}(i) + 2\gamma \sum_{n=1}^{N} e_n(k) \sum_{j=0}^{p'} c_{nm}(j)x(k-j-i) \quad (20)$$

where FIR filter of p' order, $[c_{nm}(0), c_{nm}(1), ..., c_{nm}(p')]^T$ is impulse response weights of transfer function between m-th feedforward control signal U_{Wm} and n-th residual vibration, namely the closed-loop transfer function C_{nm}. Comparison equation (20) with equation (6) informs that the proposed algorithm compensates automatically the effect of feedback link by means of the closed-loop transfer function C_{nm}. Note that impulse response weights $[c_{nm}(0), c_{nm}(1), ..., c_{nm}(p')]^T$ can be significantly less than ones of secondary plant $[h_{nm}(0), h_{nm}(1), ..., h_{nm}(p)]^T$ if feedback loop increases the damping capacity of secondary plant, and so convergence factor of the proposed algorithm γ can be set more greatly than η as deduced from equation (6), (12), (13) and (20). Therefore, hybrid active controller may be able to attenuate even transient external disturbance as illustrated in later section by numerical simulation. Additionally, calculation burden for updating hybrid controller may be reduced because closed-loop transfer function C_{nm} is modeled by FIR filter of smaller order compared to H_{nm}, i.e. $p' < p$.

2.2.2 Design of Feedback Controller

Feedback loop of hybrid controller can be designed independently of feedforward loop because feedforward controller is adapted by the proposed algorithm which compensates automatically the effect of feedback link. There are many kinds of model-based control approach available for designing the MIMO controller; e.g., optimal control, modal space control. In this research, LQG approach[6] is employed for feedback controller. Plant model including dynamic responses of primary and secondary plants is required to design feedback controller. In case that dynamic characteristics of primary plant is not feasible, the shaping filter[18] specified over main frequency components of the disturbance may be used to express primary disturbance.

If only feedback loop is used for active vibration control system, tuning of feedback controller should be focused on the reduction ratio of external disturbance which depends mainly on the sensitivity transfer function $S = (I_{N \times N} - HG)^{-1}$ as shown in equation (18). However, in case that hybrid controller is used for active vibration control system, the objectives of feedback controller are not only to improve the transient response of closed loop transfer function in order to increase the convergence rate of adaptive feedforward controller, but also to reduce persistent disturbance. Due to the fact that the summation of the sensitivity transfer function and the complimentary sensitivity transfer function is always one, this two objectives for feedback controller might be negotiated with weighting parameters related with control performance by designer.

Active vibration system including disturbance characteristics is modeled by the following discrete time state equation.

$$x(k+1) = Ax(k) + Bu(k) + Lw(k) \qquad (21)$$

$$y(k) = Cx(k) + Du(k) + n(k) \qquad (22)$$

where **A, B, C, D** and **L** are system matrices related with system states $x(k)$, control force $u(k)$, disturbance $w(k)$. $y(k)$, $n(k)$ denote the measured output and measurement noise respectively. In the LQG control, disturbance and measurement noise are assumed to be stationary, zero-mean, Gaussian white process, and to have auto-covariance matrices satisfying

$$E[w(j)w^T(k)] = Q_0\delta_{jk} , \quad E[n(j)n^T(k)] = R_0\delta_{jk} \quad (23)$$

where Q_0 and R_0 are intensities of disturbance and measurement noise respectively, and are assumed to be positive definite matrices. $E[\cdot]$ and δ_{jk} denote expected value operator and the Kronecker delta function respectively. Other cross-covariances are assumed to be nil. LQG controller is consisted of a state feedback regulator and a Kalman filter. Regulator generates control outputs by the following control law:

$$u(k) = -K x(k), \qquad (24)$$

where **K** is the state feedback gain matrix. K is determined from the following equation to minimize the performance index. $\sum_{k=0}^{\infty}[x^T(k)Qx(k) + u^T(k)Ru(k)]$

$$K = (R + B^TP_rB)^{-1}B^TP_rA \qquad (25)$$

where P_r is the solution of control algebraic Riccati equation:

$$A^TP_rA - P_r \\ \quad - A^TP_rB(R + B^TP_rB)^{-1}B^TP_rA + Q = 0 \qquad (26)$$

Q, R are both positive definite symmetric matrices allowing control designer to trade off control performance with control effort. In practice, not all state variables are available for direct measurement. In order to form the desired control vector using equation (24). it is necessary to estimate the state variables that are not directly measurable. Current type Kalman filter may be used to estimate of the all state variables based on the measured output variables:

$$\bar{x}(k+1) = A\hat{x}(k) + Bu(k) + K_e[y(k) - C\hat{x}(k) - Du(k)] \quad (27)$$

where $\hat{X}$ and K_e are the estimated state variables and gain matrix of Kalman filter respectively. Gain matrix of current type Kalman filter is determined by following equations.

$$K_e = AP_kC^T(CP_kC^T + R_0)^{-1} \qquad (28)$$

$$AP_kA^T - P_k - AP_kC^T(CP_kC^T + R_0)^{-1}CP_kA^T \\ \quad + LQ_0L^T = 0 \qquad (29)$$

The synthesis of LQG controller may be obtained by adjustments of weighting factors **Q. R**, Q_0 and R_0 repeatedly until the performance of feedback control system. such as increasing of damping capacity of the control plant and disturbance reduction over the specified frequency band, is satisfied. State feedback regulator and Kalman filter can be converted into the transfer functions of feedback controller from measured outputs to control vectors and implemented by digital filters.

3. Simulation and Experiment

3.1 Simulation and Discussion

Computer simulation is carried out in order to show which difficulties the conventional filtered-x LMS algorithm possess and how those can be overcome by the proposed algorithm.

Table 1   Computer simulation model of the secondary plant.

Zeros (z)	Poles (z)
0.9822±0.1456i	0.9742±0.1889i
0.9608	0.9902±0.0808i
gain = 0.020221	

Secondary plant is assumed to be the system with resonance at 65 Hz and 125.5 Hz as shown in Table 1. The sampling rate is selected at 5 kHz. In general, primary plant is different from secondary plant because secondary plant involves the characteristics of actuator, anti-aliasing filter and so forth, and external disturbance induced by primary source is transmitted to the sensors through different paths even though the part of the transmission paths is in common with secondary plant. For clarity of the simulation, however, it is assumed that primary plant is same with secondary plant except the added 3 step time-delay, i.e., z^{-3}. LQG feedback controller is designed with such the weights as $Q_0 = 400$, $R_0 = 1$, $Q = 400C^T C$ and $R = 1$ in the equations (23), (25) and (26). Figure 3 shows that closed-loop transfer function is significantly damped out at resonant frequencies compared to the open-loop transfer function. The convergence properties for hybrid control are investigated under the harmonic disturbance. Figure 4(a), (b) and (c) are the time histories of disturbance rejection related with feedback control, feedforward control and hybrid control in case that reference signal is consisted of sine wave of 65Hz and one of 152.5Hz changed abruptly from 0.8 second, and controller is initiated at 0.4 second. Performance of hybrid control was much better and faster compared to adaptive feedforward control and LQG feedback control. Note that even though LQG feedback controller has been designed under ideal condition, residual vibration by feedback controller cannot be eliminated completely. As described in section (3-2), convergence rates of

filtered-x LMS and proposed algorithm depend on the filtered-x signal power, $Tr(R_f)$.
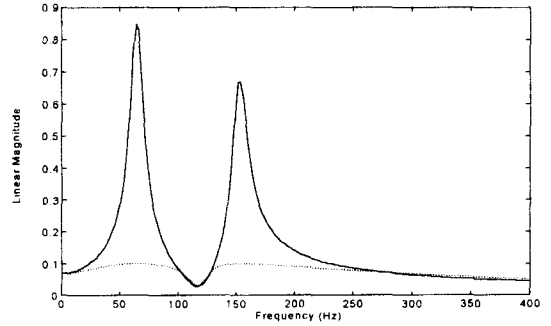

Fig. 3   Comparison between the transfer function for the secondary plant and the transfer function for the closed-loop system; ——, transfer function of the secondary plant; ----, closed-loop transfer function for the LQG feedback control system

The result of feedforward controller illustrates that filtered-x LMS algorithm yields poor transient response due to slow convergence rate.
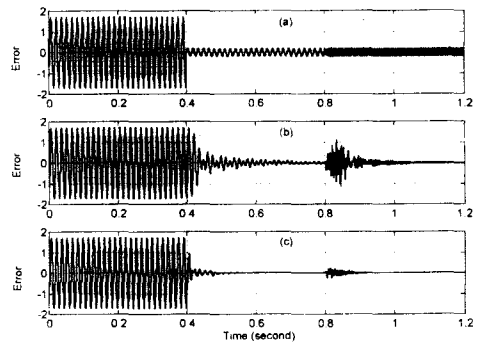

Fig. 4   Simulation for the time histories of disturbance rejection. (a) LQG feedback control; (b) FXLMS algorithm; (c) hybrid control

A comparison of $Tr(R_f)$ for filtered-x LMS and proposed algorithm, shown in figure 5, supports this result. Simulation result shows that hybrid controller is able to recover quickly from transient disturbance because of active damping component of the control signal from feedback loop, and consequently performs better for both persistent and transient disturbances.

3.2 Expeiment and Discussion
3.2.1 Experimental Set-up

Figure 6 is the schematic diagram of the active trim panel, inertial type actuator, and an experimental set-up that simulates structure-bone excitation. The active trim panel is mounted to the stiffening members of a aircraft fuselage skin via soft mounts and a lightweight, acoustically unobtrusive, aluminum frame.
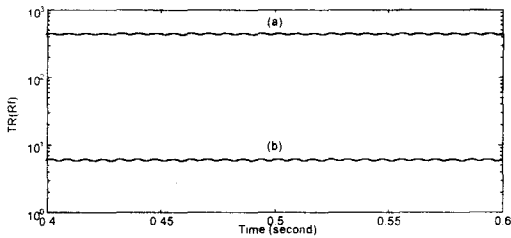

Fig. 5 Comparison of $Tr(R_f)$ between FXLMS algorithm and the proposed algorithm. (a) FXLMS algorithm: (b) proposed algorithm.

The active trim panel is placed on top of a layer of passive absorbing fiber glass in order to reduce the high frequency vibration component. Trim panel is a $45.7 \times 45.7 \times 2.54\ cm^3$ honeycomb composite consisting of a $2.54\ cm$ aluminum core and carbon fiber face sheets on either side.
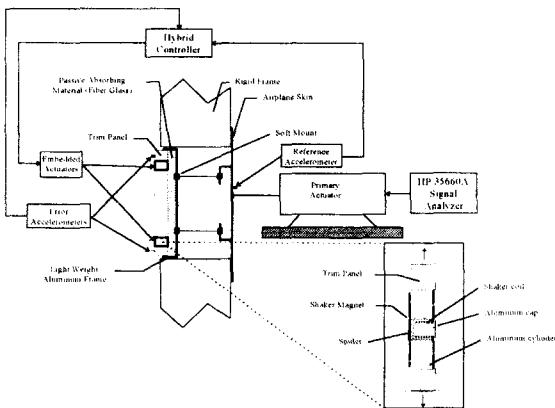

Fig. 6 Schematic diagram of the active trim panel, inertial type actuator, and an experimental set-up that simulates structure-bone excitation

The trim panel weighs $1.59\ kg_f$ and has the first bending mode at approximately 530Hz after combined with passive absorbing material and aluminum frame. An inertial type actuator and accelerometer(PCB, 303A02) are embedded near each of the 4 corners of trim panel to generate control forces and measure the vibration level. These actuator consist of a shaking coil which is mounted rigidly to the panel, and a magnet part which is free to move in and out-of-plane motion using circular spider. Each actuator produces approximately 0.7 N force over 50 to 500Hz bandwidth when 1 volt random signal is inputted.

Digital controller for active vibration control of trim panel is conducted by a digital signal processor (Spectrum QPC40) which consists of 4 floating-point microprocessors (Texas Instrument, TMS320C40) capable of parallel signal processing, 12-bit 5 channel A/D converters, and 12-bit 4 channel D/A converters. An electromagnetic shaker (VTS VG600 Vibrator) is attached the skin plate in order to generate the external disturbance. 4 anti-aliasing filters, which are set at 1250 Hz, are used so that high frequency component from D/A converters is eliminated. A signal analyzer (HP35660) evaluates the control performance of realized system and provides the pseudo-random source.

3.2.2 Experimental Results

For the design of hybrid controller, 16 frequency transfer functions for secondary plant were measured using the signal analyzer and then a 4×4 MIMO ARMA (auto-regressive moving average) model whose order is 29, is identified based on frequency domain curve fitting[19] and balanced minimum realization[20]. This fitting method is capable of avoiding window distortion and system identification in one step due to the matrix-fraction approach of Markov parameter. Figure 7 shows the transfer functions related with only the 4th inertial actuator which are measured and identified. Note that this secondary plant represents all dynamic characteristics from inertial actuators to accelerometers including amplifiers, vibration transmission paths, anti-aliasing filters, time-delay of digital signal processor and so forth. The first resonance at 65Hz is due to circular spider of inertial actuator itself. The second resonance at 350Hz is due to suspension between trim panel and

skin plate of aircraft fuselage. The third resonance at 530Hz is due to first bending mode of trim panel. By using impact hammer instead of the inertial actuator, two rocking modes at 7.75Hz and 8.25 Hz, and one piston-like mode at 9Hz were certified. These rigid-body modes were highly damped due to the fiber-glass absorbing material and the rubber joints installed between trim panel and skin plate. It should be noted that the low frequency noise fields below 50Hz, induced by forced vibration components of trim panel, are not usually active control objects because of insensitivity of humans.

The LQG feedback controller was designed based on the identified MIMO model. The weights for designing LQG controller were selected as follows:

$$Q = 15 \times C^T C . Q_0 = \begin{bmatrix} 15 & 6 & 6 & 6 \\ 6 & 15 & 6 & 6 \\ 6 & 6 & 15 & 6 \\ 6 & 6 & 6 & 15 \end{bmatrix}$$

$$\text{and} \quad R = R_0 = \begin{bmatrix} 1 & 0.4 & 0.4 & 0.4 \\ 0.4 & 1 & 0.4 & 0.4 \\ 0.4 & 0.4 & 1 & 0.4 \\ 0.4 & 0.4 & 0.4 & 1 \end{bmatrix}.$$

These weights were determined, under the consideration of the ratios between amplitudes of the direct transfer functions e.g., H_{11}, H_{22} and the one of cross transfer functions, e.g., H_{12}, H_{13} of the identified secondary model, so that closed loop transfer functions maintain as symmetrically as possible.

Comparison of open-loop transfer function and closed-loop transfer function as shown in Figure 7 (dashed-line) illustrates that the feedback loop decreased the resonant response of secondary plant considerably. Figure 8 shows the experimental results for the active vibration control system. Broadband external vibration up to 630Hz could be attenuated by 5-20dB in the vibration level. Note that the external forced vibration of trim panel, induced by the primary actuator(shaker), consists of 4 vibration modes, namely 3 rigid body and 1 bending vibrations. The inefficiency with low frequency

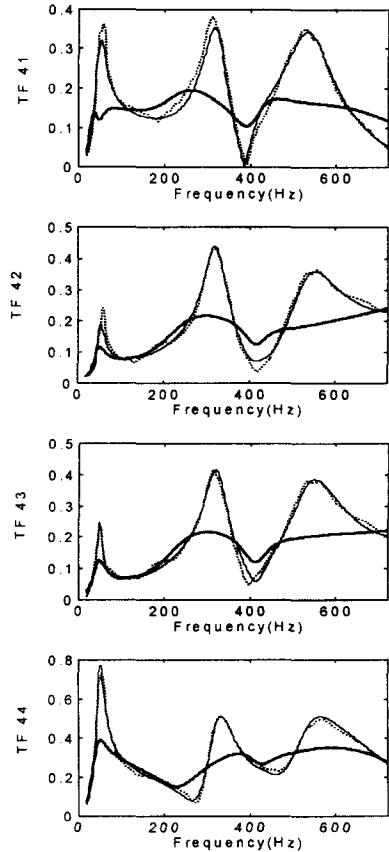components below 50Hz may be ascribed to the power limit of inertial actuator.

Fig. 7 Frequency response functions for the secondary plants. ·····, experimental measured frequency response functions; ——, mathematical models; ----, simulated closed-loop transfer functions

Sampling rate was at 2kHz considering the frequency bandwidth of disturbance, and the calculation burden of digital signal processor. FIR filter of 120 order was used for the feedforward controller and adapted by proposed algorithm. Closed loop transfer function of secondary plant was in the form of FIR filter of 60 order required coefficients due to increased damping ratio by feedback path. As the time histories of residual at the first accelerometer shown in figure 9, hybrid controller, whose the convergence factor was set at 0.001, was converged in 2 seconds.
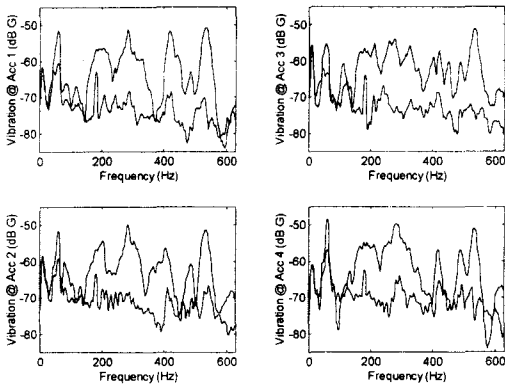
Fig. 8 Vibration reduction at 4 accelerometer locations;
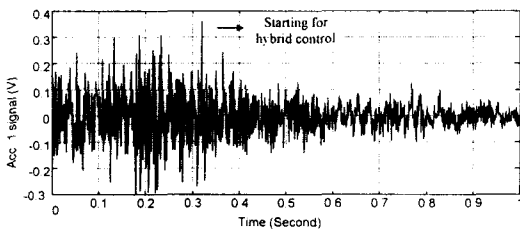----, without control; ———, with hybrid control

Fig. 9 Time history of the active panel system with
hybrid controller

4. Conclusion

Active vibration control system to reduce the sound
transmission through trim panel has been presented. It
is effective for attenuation of broad band vibration
induced by external source. The problem related with
adaptive feedforward controller is analyzed theoretically
in the viewpoint of convergence rate especially when
secondary plant has the resonant response characteristics.
To solve this problem, the hybrid control loop which
consists of an adaptive feedforward and a LQG feedback
control, and the related adaptation rule is described.
Hybrid controller for active trim panel is applicable to
both persistent and transient external vibrations due to
the high rate convergence. The actual implementation
of MIMO controller for active trim panel, which is

designed as prototype of aircraft fuselage, shows that
approximately 12dB reduction in the vibration level of
trim panel over the 50~600Hz broadband can be
achieved.

References

1. S. J. Sharp, G. H. Koopmann, and W. Chen,
   "Transmission loss characteristics of an active trim
   panel," '97 Proceedings of Noise-Con Book 2,
   pp.149-160, 1997.
2. C. R. Fuller, "Active control of sound
   transmission/radiation from elastic plates by
   vibration inputs: I. Analytical study," Journal of
   Sound and Vibration, Vol.136, pp.1-15, 1990.
3. D. R. Thomas, P. A. Nelson, R. J. Pinnington, and S.
   J. Elliott, "An analytical investigation of the active
   control of the transmission of sound through plates,"
   Journal of Sound and Vibration Vol.181, pp.515-
   539, 1995.
4. R. L. St. Pierre, Jr., W. Chen and G. H. Koopmann,
   "Design of adaptive panels with high transmission
   loss characteristics," 2nd AIAA/CEAS Aeronautics
   Conference AIAA 96-1700. 1996.
5. L. Meirovitch and H. Baruh, "Control of self-
   adjoint distributed-parameter systems," Journal of
   Guidance Control, Vol.5, pp.59-66, 1982.
6. R. Shoureshi, L. Brackney, N. Kubota and G. Batta,
   "A modern control approach to active noise control,"
   ASME Journal of Dynamic Systems, Measurement,
   and Control, Vol.115, pp.673-678. 1993.
7. B. A. Francis, A course in H_x Control Theory,
   New York: Springer-Verlag, 1986.
8. J. C. Burgess, "Active adaptive sound control in a
   duct: A computer simulation," Journal of Acoustical
   Society of America, Vol.70, pp.715-725, 1981.
9. L. J. Eriksson, M. C. Allie and R. A. Greigner, "The
   selection and application of an IIR adaptive filter for
   use in active sound attenuation," IEEE Transaction
   on Acoustics, Speech and Signal Processing, Vol.35,
   pp.433-437, 1987.
10. S. D. Snyder and C. H. Hansen, "The influence of
    transducer transfer functions and acoustic time

delays on the implementation of the LMS algorithm in active noise control system," Journal of Sound and Vibration, Vol.141, pp.409-424, 1990.

11. I. S. Kim, H. S. Na, K. J. Kim and Y. Park, "Constraint filtered-x and filtered-u least-mean-square algorithms for the active control of noise in ducts," Journal of Acoustical Society of America, Vol.95, pp.3379-3389, 1994.

12. W. R. Saunders, H. H. Robertshaw and R. A. Burdisso, "A hybrid structural control approach for narrow-band and impulsive disturbance rejection," Noise Control Engineering Journal, Vol.44, pp.11-21, 1996.

13. Y. R. Ho, I. S. Kim, W. Chen and G. H. Koopmann, "Active control of broadband sound transmission using feedback and feedforward techniques," '97 Proceedings of Noise-Con Book 2, pp.161-172, 1997.

14. P. A. Nelson and S. J. Elliott, Active control of sound, San Diego, California: Academic Press, 1992.

15. W. R. Saunders, H. H. Robertshaw, and R. A. Burdisso, "A hybrid structural control approach for narrow-band and impulsive disturbance rejection," Noise Control Engineering ,Vol.44, pp.11-21, 1996.

16. G. C. Goodwin and K. S. Sin, Adaptive Filtering Prediction and Control, New York: Prentice-Hall, 1984.

17. B. Widrow and S. D. Sterns, Adaptive Signal Processing, New York: Prentice-Hall, 1985.

18. W. T. Baumann, F. S. Ho and H. H. Robertshaw, "Active structural acoustic control of broadband distrubances," Journal of Acoustical Society of America, Vol.92, 1998-2005, 1992.

19. J. N. Juang, Applied System Identification, Englewood Cliffs, New Jersey: Prentice Hall, 1994.

20. K. Zhou, J. C. Doyle and K. Glover, Robust and Optimal Control, Upper Saddle River, New Jersey: Prentice Hall, 1996.